Supplement of Atmos. Chem. Phys., 26, 3467–3487, 2026
https://doi.org/10.5194/acp-26-3467-2026-supplement

Atmospheric Chemistry and Physics
Open Access
EGU

Supplement of

Measurement report: Three-year characteristics of sulfuric acid in urban Beijing and derivation of daytime sulfuric acid proxies applicable to inland sites

Yishuo Guo et al.

Correspondence to: Chao Yan (chaoyan@nju.edu.cn) and Yongchun Liu (liuyc@buct.edu.cn)

Section S1. Measurement at Hyytiälä site

The boreal forest SMEAR II station is located at Hyytiälä, southern Finland (Hari and Kulmala, 2005;Hari et al., 2013). The datasets used in this study are from 8th March to 13th August in 2018.

Sulfuric acid was measured by a CI-APi-TOF mass spectrometry using nitric acid as reagent ions at the top of a 35 m tower. The calibration coefficient of sulfuric acid during the measurement period was 3.2×10^9 molec cm^{-3}. UVB radiation was also measured at the same height as sulfuric acid by a radiometer (Solar Light SL501A). The particle number distributions of 3 - 1000 nm aerosols were obtained by a twin differential mobility particle sizer (DMPS) (Aalto et al., 2001) at 8 m in height above ground, and was then used to calculate the condensation sink (CS) according to the method from Kulmala et al. (Kulmala et al., 2001;Kulmala et al., 2012;Kerminen et al., 2001) Besides, meteorological parameters and trace gases were continuously monitored at various heights (4.2, 8.4, 16.8, 33.6, 50.4, 67.2, 101, and 125 m) on a 126 m mast. Air temperature was measured by PT-100 resistance thermometer, and air relative humidity (RH) was monitored by RH sensor (Rotronic HygroMet MP102H with HygroClip HC2S3, Rotronic AG, Switzerland). SO_2 mixing ratio was monitored using an SO_2 fluorescence analyzer (Model 43i, Thermo, USA). The temperature, RH and SO_2 measured at 33.6 m were utilized to match the height of sulfuric acid and UVB.

Section S2. Estimation of hourly $PM_{2.5}$ for Hyytiälä site

The mass concentrations of $PM_{2.5}$ and PM_{10} of Hyytiälä were continuously measured with the filter-sampled Impactor, but they only had a resolution of 1–3 days. Meanwhile, the PM_{10} was additionally monitored by a SHARP instrument with hourly resolution. Therefore, it is possible to obtain the hourly $PM_{2.5}$ data from hourly PM_{10}. We then explore the relationship between $PM_{2.5}$ and PM_{10} from Impactor measurement. And as shown in Figure S12B, $PM_{2.5}$ had a very good linear correlation (R = 1.0) with PM_{10} and the scaling factor between them was 0.8. Thus, we calculated the hourly $PM_{2.5}$ based on the equation of $PM_{2.5} = 0.8 \times PM_{10}$.

Section S3. Uncertainty analysis of sulfuric acid proxies

According to equation (4), the uncertainty of OH-CS based proxy can be calculated as follows:

$$E_{Proxy_{OH,CS}} = \sqrt{(-0.7)^2 \cdot (E_T)^2 + \left(E_{SO_2}\right)^2 + (E_{OH})^2 + (-1)^2 \cdot (E_{CS})^2}$$

The relationship between OH radical and UVB is $OH = 6.14 \times 10^6 \cdot UVB$. Then the uncertainty of replacing OH radical by UVB is:

$$E_{UVB\text{-}substitution} = \sqrt{(E_{UVB\text{-}measure})^2 + (E_{UVB\text{-}to\text{-}OH})^2 + \left(E_{OH\text{-}modelling}\right)^2}$$

The relationship between CS and $PM_{2.5}$ is $CS = 2.67 \times 10^{-3} \cdot PM_{2.5}^{2/3}$. Then the uncertainty of replacing CS by $PM_{2.5}$ is:

$$E_{PM_{2.5}\text{-}substitution} = \sqrt{(2/3)^2 \cdot \left(E_{PM_{2.5}\text{-}measure}\right)^2 + \left(E_{PM_{2.5}\text{-}to\text{-}CS}\right)^2 + (E_{CS})^2}$$

The accuracies of measuring temperature (Vaisala) and $PM_{2.5}$ (ThermoFisher) are usually smaller than 1% , and therefore can be ignored. The accuracies of measuring SO_2 (ThermoFisher) and UVB (KIPP&ZONEN) are around 1% and 5% respectively. The uncertainty of the model calculations of OH radical is approximately 40% (Tan et al., 2017;Ma et al., 2019;Ma et al., 2022). The underestimation of CS from DMPS measurement is around 11.7% (Figure S14, averaged relative errors of three periods). The relative error of using UVB to substitute OH radical is 86.5% (Figure S7A), and the relative error of using $PM_{2.5}$ to substitute CS is 28.9% (Figure S7B). Bring those uncertainties of parameters into the above equations, we can get:

$$E_{UVB\text{-}substitution}=\sqrt{(E_{UVB\text{-}measure})^2+(E_{UVB\text{-}to\text{-}OH})^2+\left(E_{OH\text{-}modelling}\right)^2}=\sqrt{(5\%)^2+(86.5\%)^2+(40\%)^2}=95.4\%$$

$$E_{PM_{2.5}\text{-}substitution}=\sqrt{\left(E_{PM_{2.5}\text{-}to\text{-}CS}\right)^2+(E_{CS})^2}=\sqrt{(28.9\%)^2+(11.7\%)^2}=31.2\%$$

$$E_{Proxy_{OH,CS}}=\sqrt{\left(E_{SO_2}\right)^2+(E_{OH})^2+(E_{CS})^2}=\sqrt{(1\%)^2+(40\%)^2+(11.7\%)^2}=41.7\%$$

$$E_{Proxy_{UVB,CS}}=\sqrt{\left(E_{SO_2}\right)^2+(E_{UVB\text{-}substitution})^2+(E_{CS})^2}=\sqrt{(1\%)^2+(95.4\%)^2+(11.7\%)^2}=96.1\%$$

$$E_{Proxy_{UVB,PM_{2.5}}}=\sqrt{\left(E_{SO_2}\right)^2+(E_{UVB\text{-}substitution})^2+\left(E_{PM_{2.5}\text{-}substitution}\right)^2}=\sqrt{(1\%)^2+(95.4\%)^2+(31.2\%)^2}=100.4\%$$

In summary, the uncertainties of OH-CS, UVB-CS and UVB-$PM_{2.5}$ based proxies are estimated to be 41.7%, 96.1% and 100.4%, respectively.

Figures

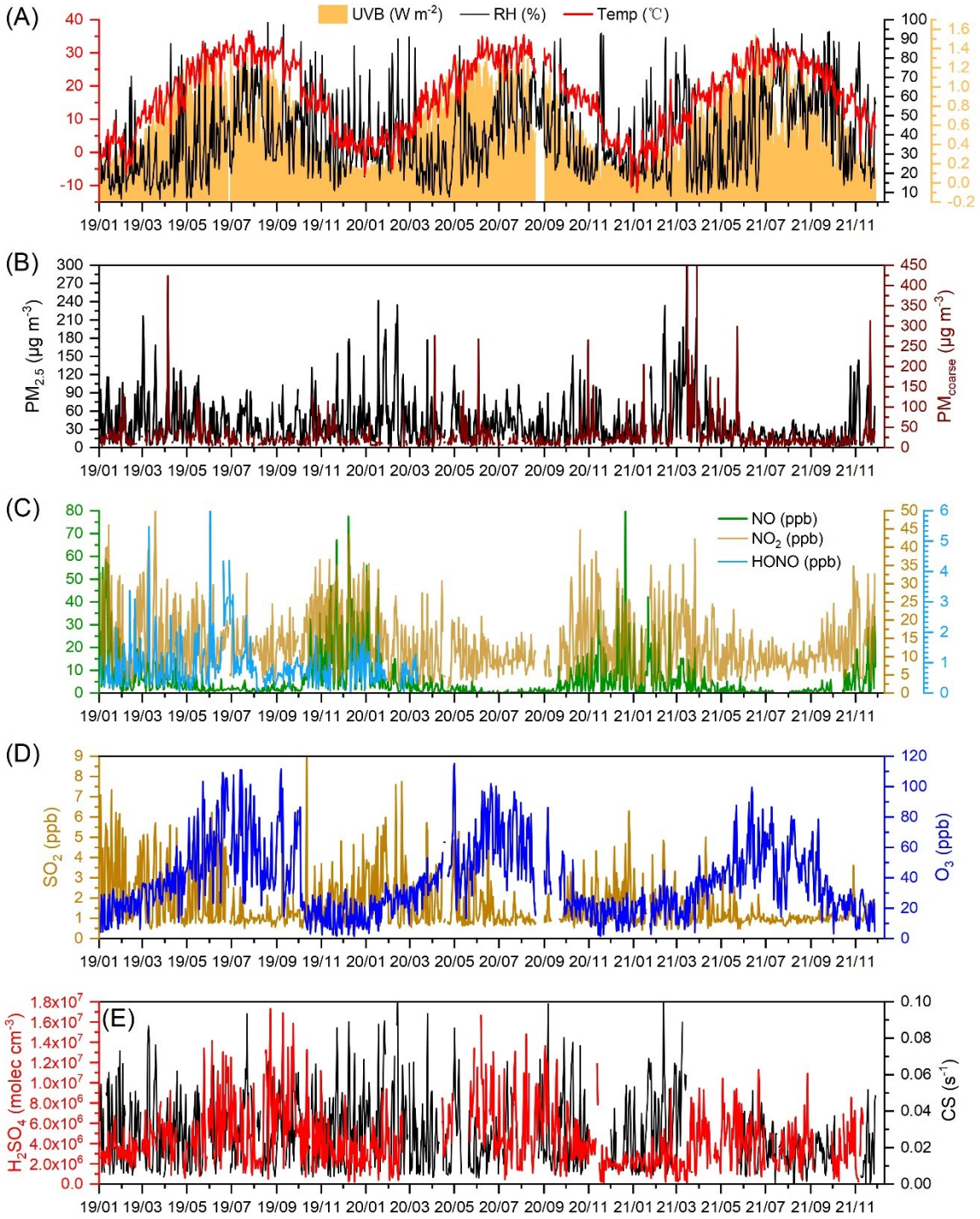

Figure S1. Three-year (from 2019 to 2021) time variations of (A) UVB, RH and temperature, (B) $PM_{2.5}$ and PM_{coarse}, (C) NO, NO_2 and HONO, (D) SO_2 and O_3, and (E) sulfuric acid (H_2SO_4) and condensation sink (CS) during daytime (10:00-14:00). The labels on x-axes are in "year/month" format.

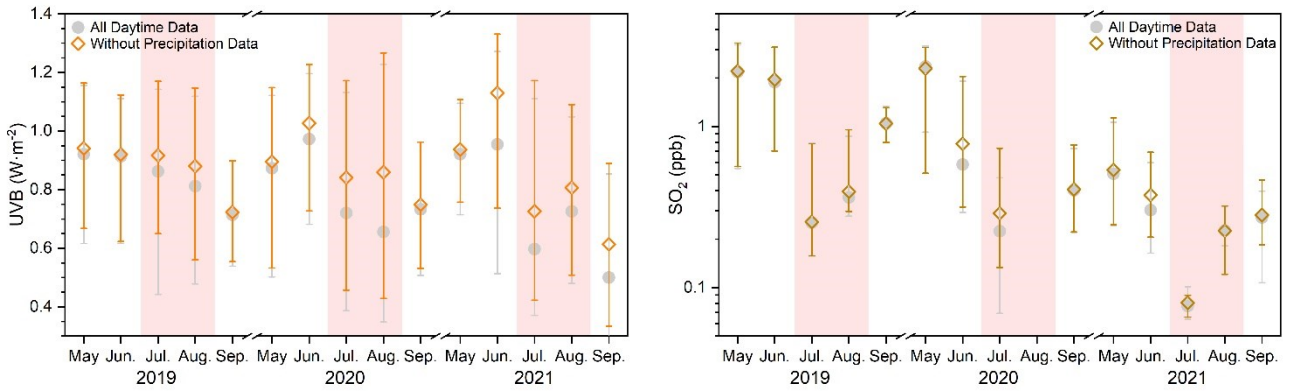

Figure S2. Monthly variations of UVB and SO_2 during daytime (10:00-14:00) in May, June, July, August and September in 2019, 2020 and 2021. The gray circles and orange diamonds represents datasets of all and without precipitation moments, respectively. The up line, middle marker and bottom line stand for upper quartile, median and lower quartile values respectively.

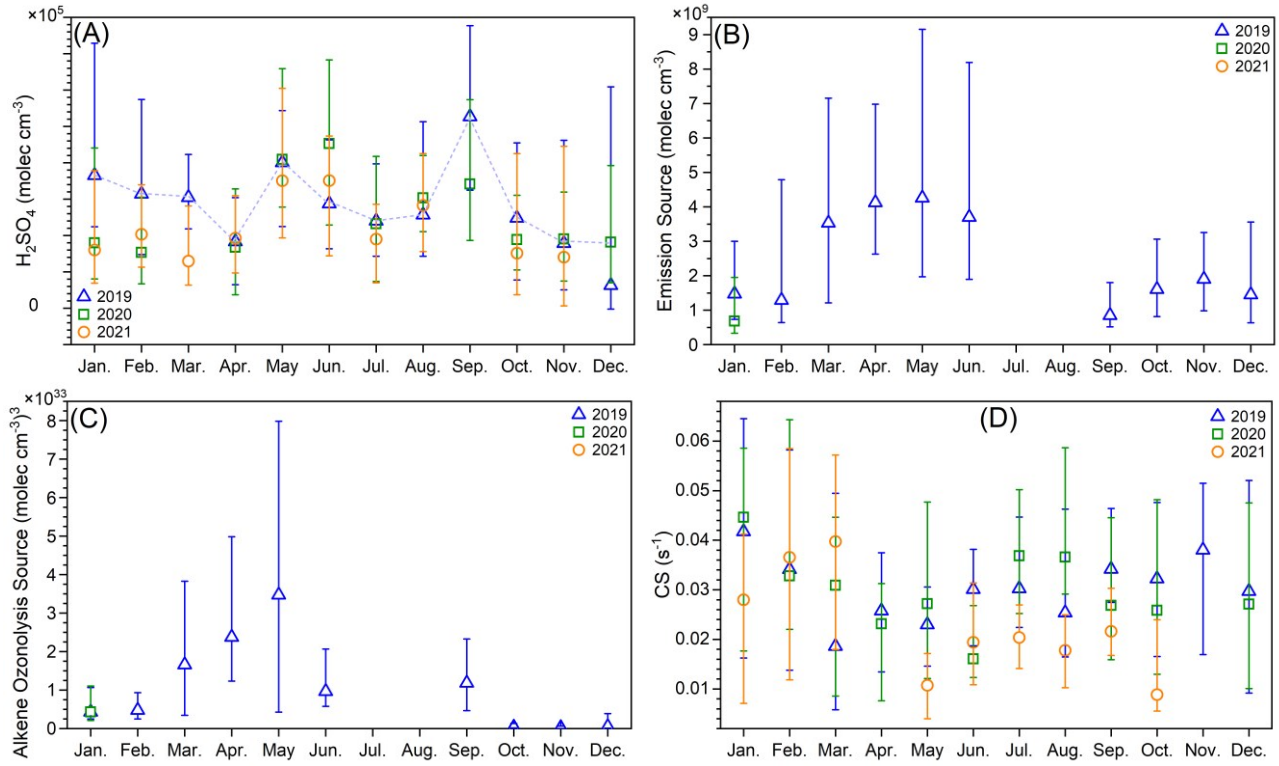

Figure S3. Three-year (from 2019 January to 2021 November) monthly variations of (A) H_2SO_4 concentration, (B) emission source of H_2SO_4 (Emission Source=[Benzene]$(\frac{WS}{1\ m\ s^{-1}})^{1.398}(\frac{CS}{0.01\ s^{-1}})^{-1.404}$ (Yang et al., 2021)), (C) alkene ozonolysis source of H_2SO_4 (Alkene Ozonolysis Source=$[SO_2][O_3]$[Alkene] (Guo et al., 2021)) and (D) condensation sink (CS) during nighttime (22:00-02:00 next day). Blue triangles, green squares and orange circles represent data in 2019, 2020 and 2021, respectively. The up line, middle marker and bottom line stand for upper quartile, median and lower quartile values, respectively.

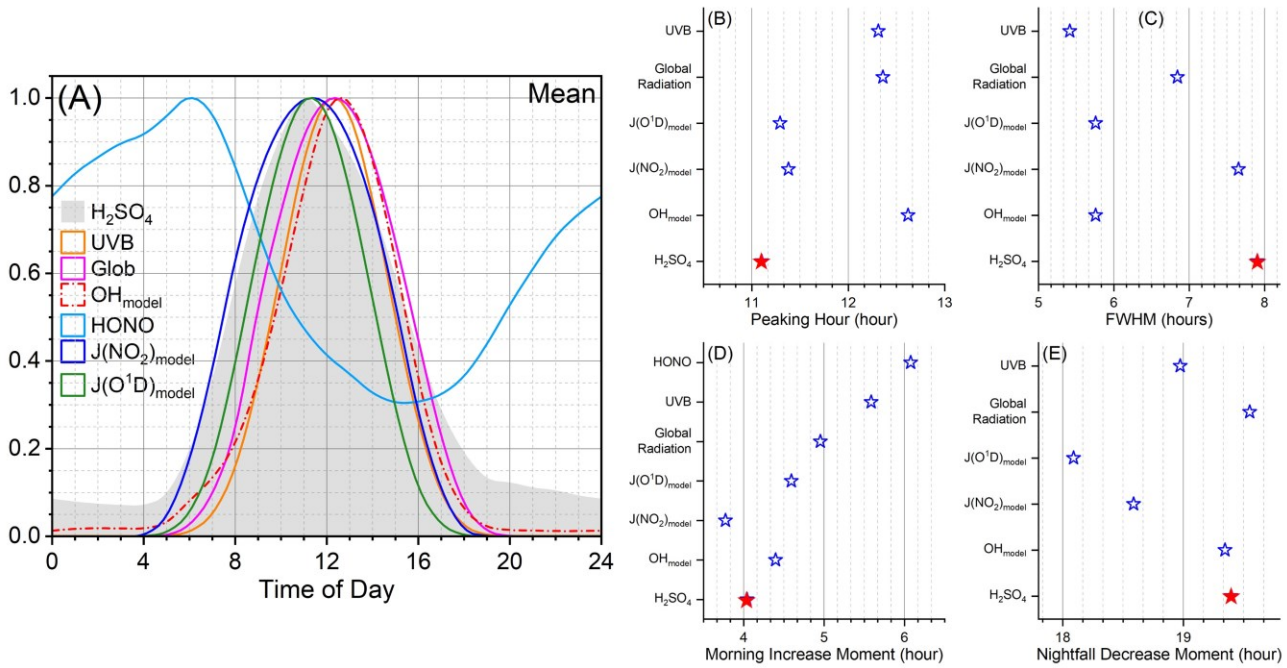

Figure S4. (A) Mean diurnal variations of H_2SO_4, UVB, global radiation (Glob), modelled OH radical (OH_{model}), HONO, modelled photolysis rate of NO_2 ($J(NO_2)_{model}$) and modelled photolysis rate of O_3 to generate $O(^1D)$ ($J(O^1D)_{model}$) of 2019. The diurnal curves are depicted in normalized values. Values of (B) peaking hour, (C) full width at half maximum (FWHM), (D) morning increase moment, and (E) nightfall decrease moment from the curves of figure (A). Except from HONO, morning increase moment is when the diurnal curve starts increasing rapidly in the morning, and the nightfall decrease moment is when the diurnal curve turns from rapid to slow decreases at nightfall. For HONO, the "morning increase moment" is when HONO starts declining rapidly in the morning.

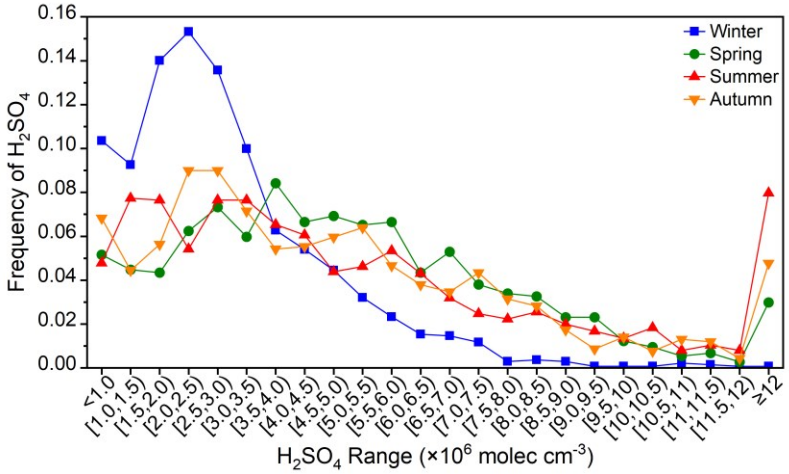

Figure S5. Distribution of daytime (10:00-14:00) sulfuric acid concentration in four seasons during three years (2019 to 2021).

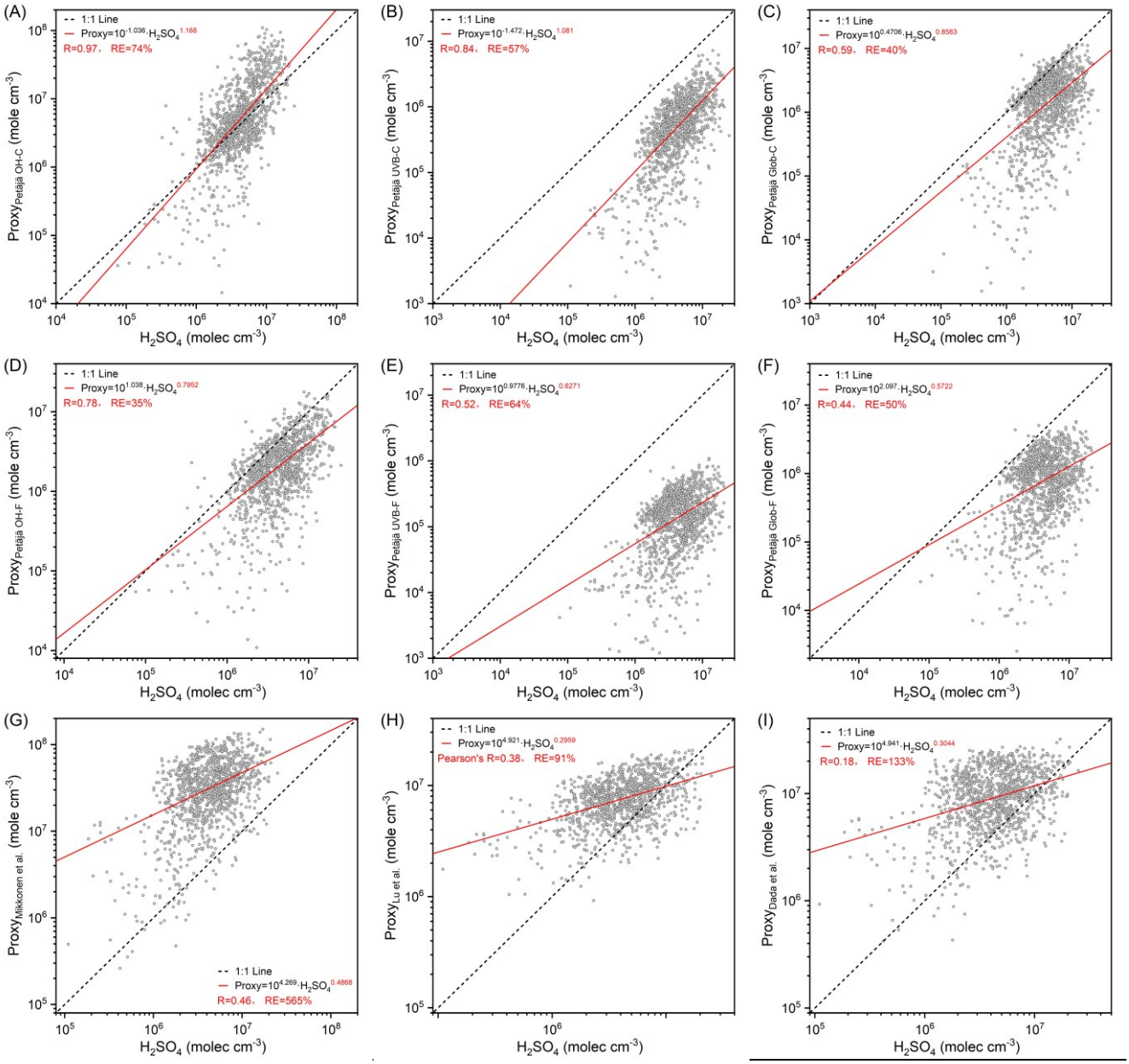

Figure S6. H_2SO_4 proxy suggested by (A) Petäjä et al., 2009 using OH radical with constant pre-factor k_1, (B) Petäjä et al., 2009 using UVB with constant pre-factor k_2, (C) Petäjä et al., 2009 using global radiation with constant pre-factor k_3, (D) Petäjä et al., 2009 using OH radical with fitted pre-factor k_1, (E) Petäjä et al., 2009 using UVB with fitted pre-factor k_2, (F) Petäjä et al., 2009 using global radiation with fitted pre-factor k_3 , (G) Mikkonen et al., 2011 with equation N5, (H) Lu et al., 2019 with equation N7 , and (I) Data et al., 2020 with the result of Figure 7(b) vs. measured H_2SO_4 during daytime (10:00-14:00) in 2019. In each plot, the black dashed lines are 1:1 lines, and the red lines are the least square fit lines between proxy and measured H_2SO_4. Corresponding functions of the least square fit, correlation coefficients (R), and the relative error (RE) between proxies and measured H_2SO_4 are also shown in the legend.

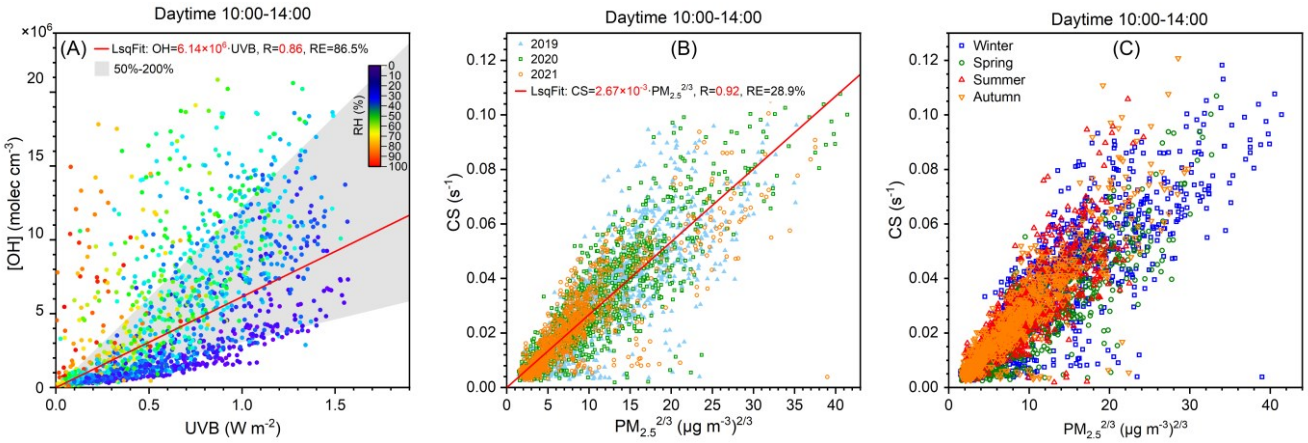

Figure S7. (A) Relationship between modelled OH radical and UVB colored by RH during daytime (10:00-14:00) in 2019. (B) and (C) Relationship between condensation sink (CS) and $PM_{2.5}^{2/3}$ during daytime from 2019 to 2021. In figure B, light blue triangle, hollow green square and hollow orange circle are for 2019, 2020 and 2021, respectively. In figure C, blue square, green circle, red upper triangle and orange lower triangle are for winter, spring, summer and autumn, respectively. Red lines are the least square fit lines between two parameters. The corresponding functions, correlation coefficients (R) and relative errors (RE) are shown in the legend. Gray area in figure A denotes 50% to 200% of the least square fitting.

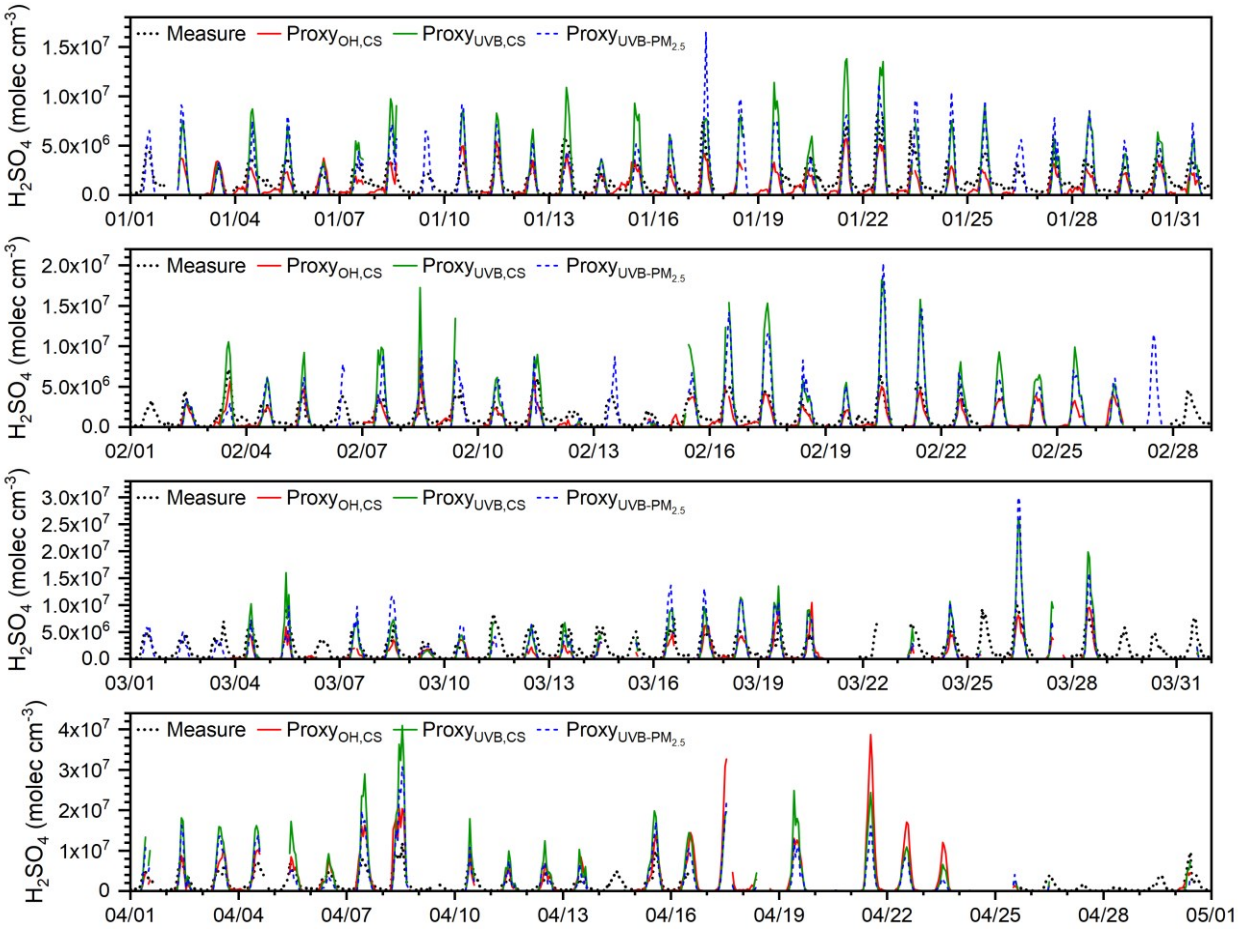

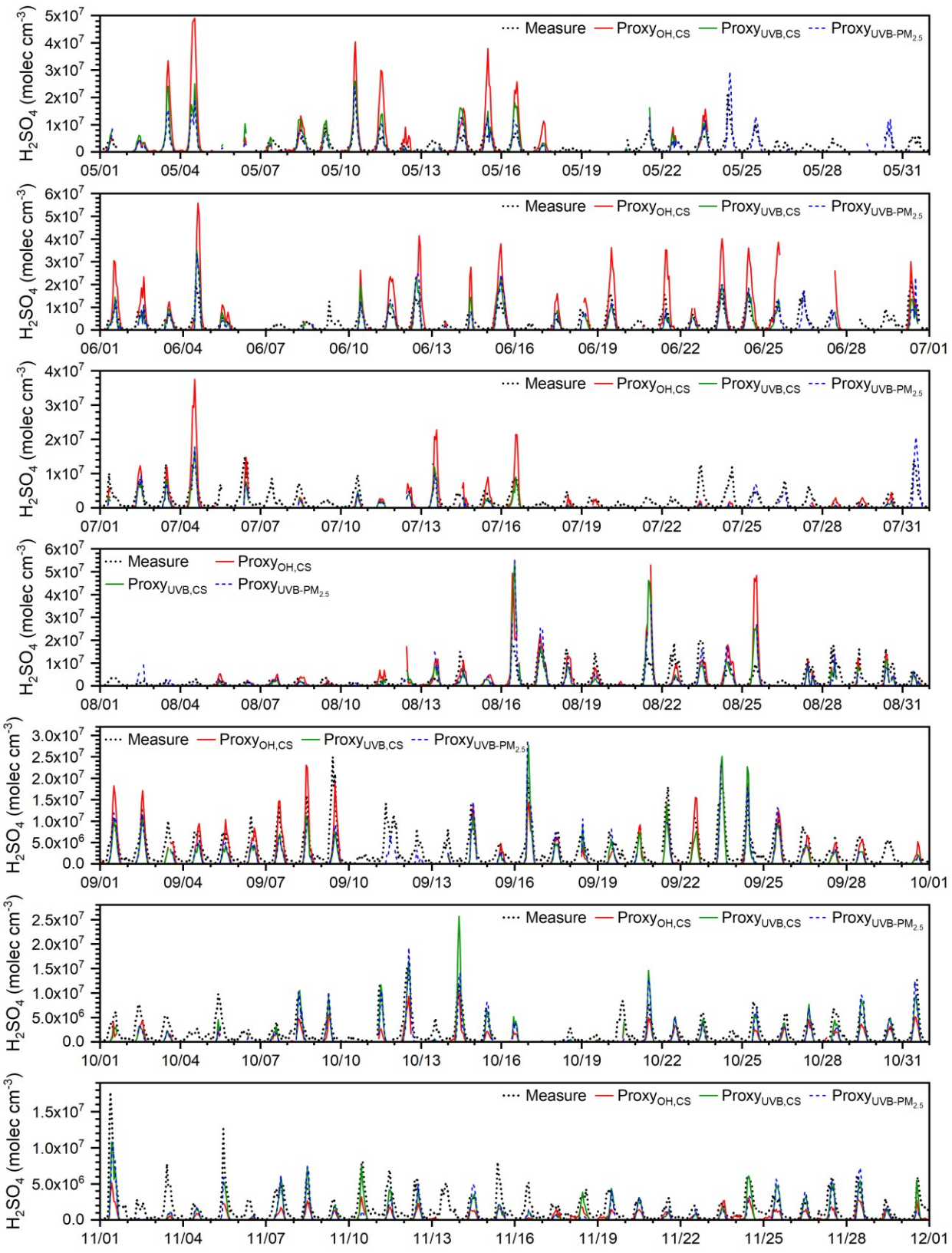
Measure
Proxy$_{OH,CS}$
Proxy$_{UVB,CS}$
Proxy$_{UVB-PM_{2.5}}$
H_2SO_4 (molec cm^{-3})
05/01 05/04 05/07 05/10 05/13 05/16 05/19 05/22 05/25 05/28 05/31
06/01 06/04 06/07 06/10 06/13 06/16 06/19 06/22 06/25 06/28 07/01
07/01 07/04 07/07 07/10 07/13 07/16 07/19 07/22 07/25 07/28 07/31
08/01 08/04 08/07 08/10 08/13 08/16 08/19 08/22 08/25 08/28 08/31
09/01 09/04 09/07 09/10 09/13 09/16 09/19 09/22 09/25 09/28 10/01
10/01 10/04 10/07 10/10 10/13 10/16 10/19 10/22 10/25 10/28 10/31
11/01 11/04 11/07 11/10 11/13 11/16 11/19 11/22 11/25 11/28 12/01

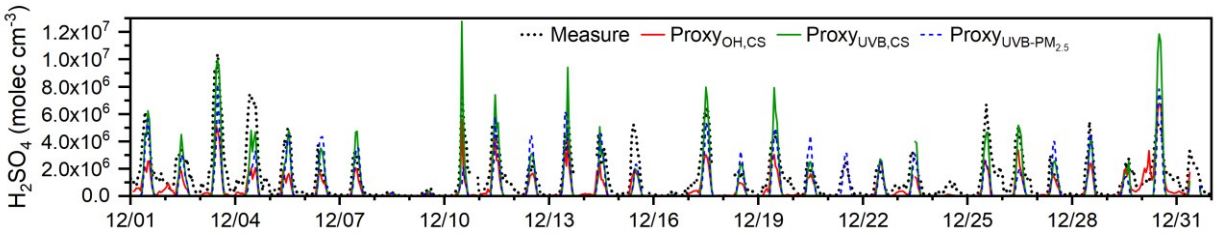

Figure S8. Time variation of measured sulfuric acid (Measure, black dashed line), OH-CS based proxy (Proxy$_{OH,CS}$, red line), UVB-CS based proxy (Proxy$_{UVB,CS}$, green line) and UVB-PM$_{2.5}$ based proxy (Proxy$_{UVB,PM_{2.5}}$, blue dashed line) of sulfuric acid in 2019.

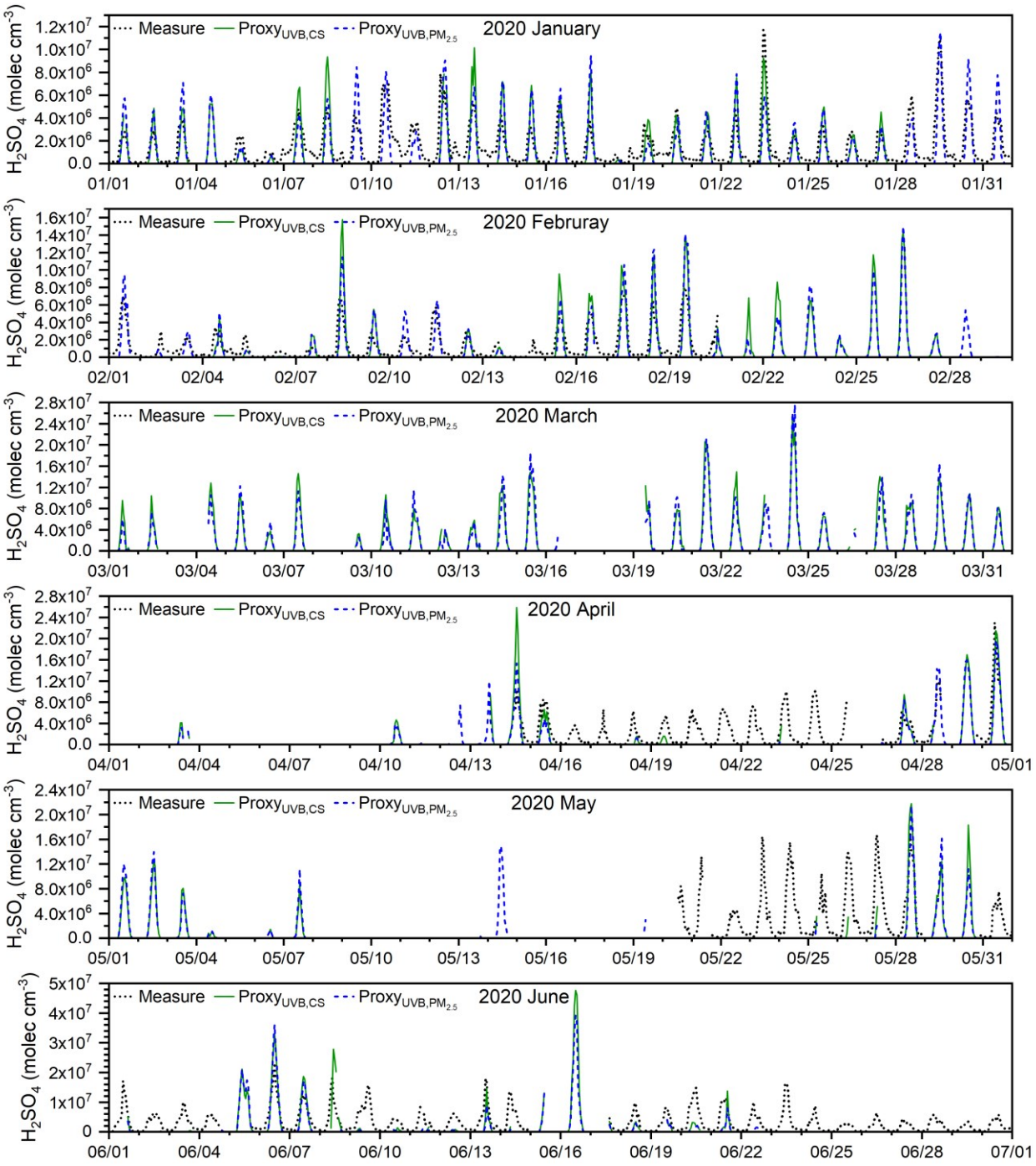

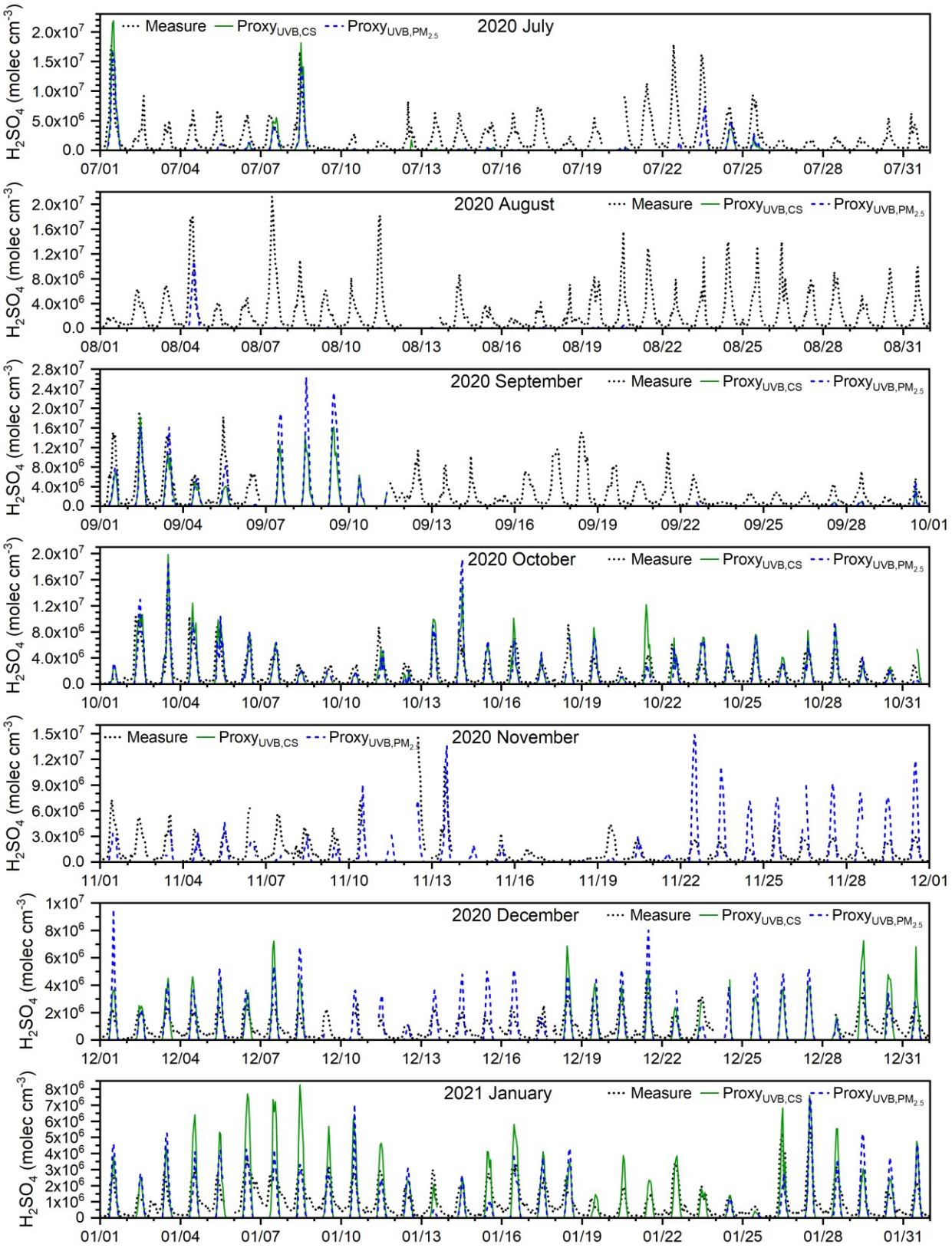
Measure
Proxy$_{UVB,CS}$
Proxy$_{UVB,PM_{2.5}}$
2020 July
2020 August
2020 September
2020 October
2020 November
2020 December
2021 January
H_2SO_4 (molec cm^{-3})

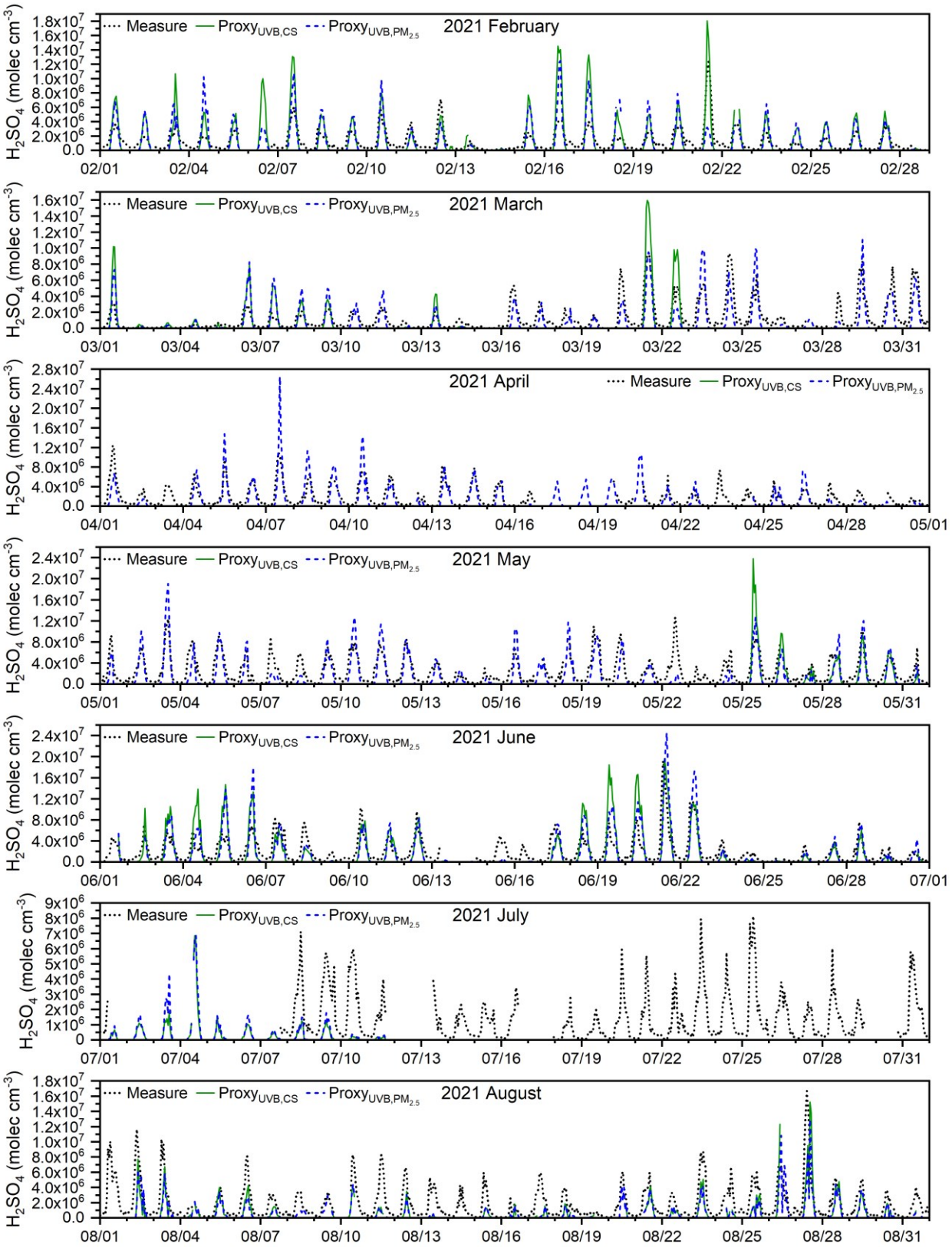
Measure
Proxy$_{UVB,CS}$
Proxy$_{UVB,PM_{2.5}}$
2021 February
2021 March
2021 April
2021 May
2021 June
2021 July
2021 August
H_2SO_4 (molec cm^{-3})

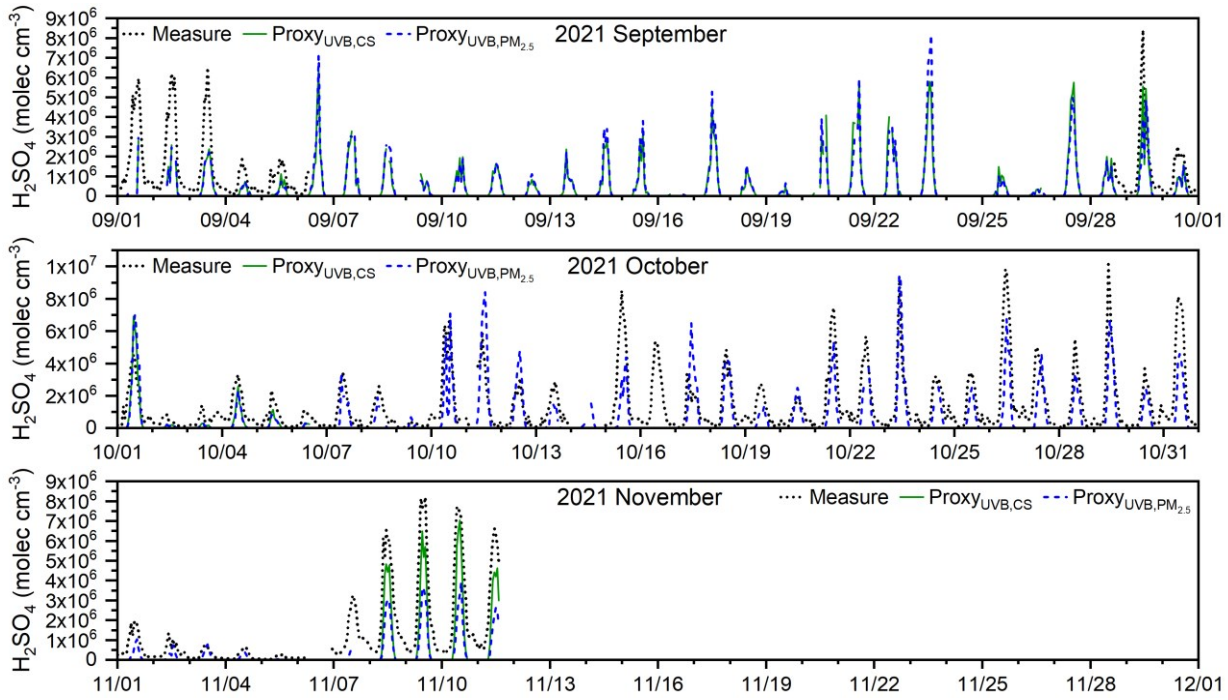

Figure S9. Time variations of measured sulfuric acid (Measure, black dashed line), UVB-CS based proxy (Proxy$_{UVB,CS}$, green line) and UVB-PM$_{2.5}$ based proxy (Proxy$_{UVB,PM_{2.5}}$, blue dashed line) of sulfuric acid in 2020 and 2021.

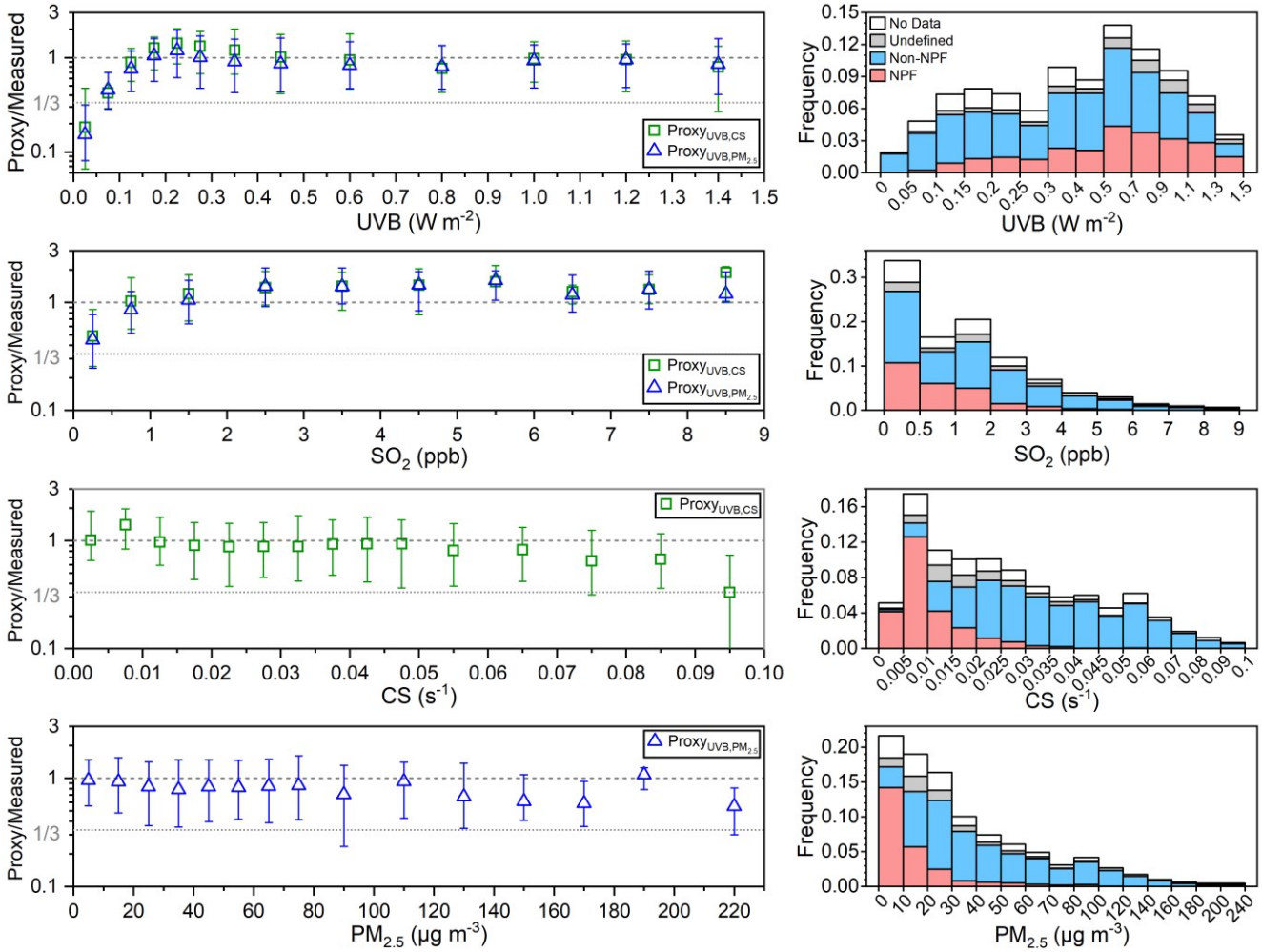

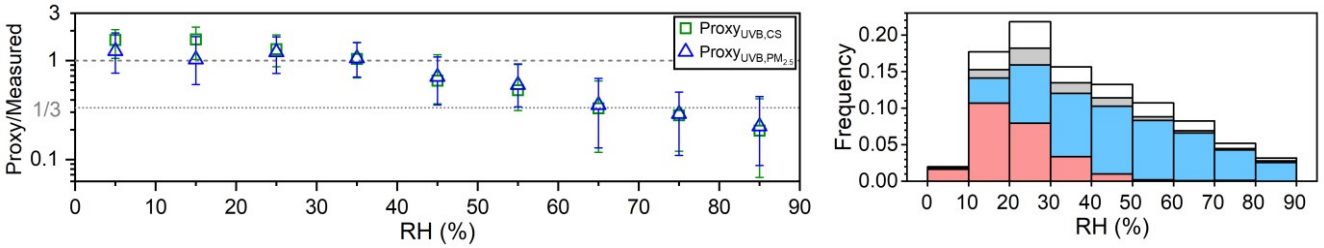

Figure S10. Left: The ratios of sulfuric acid concentrations estimated by proxies in this study to the measured one (Proxy/Measured) vs. UVB, SO_2, CS, $PM_{2.5}$ and RH during daytime (10:00-14:00) of three years. Different colored markers represent different proxies. The up line, middle marker and bottom line stand for upper quartile, median and lower quartile values respectively. Right: Frequency distributions of corresponding parameters classified by "NPF", "Non-NPF", "Undefined", and "No Data" periods.

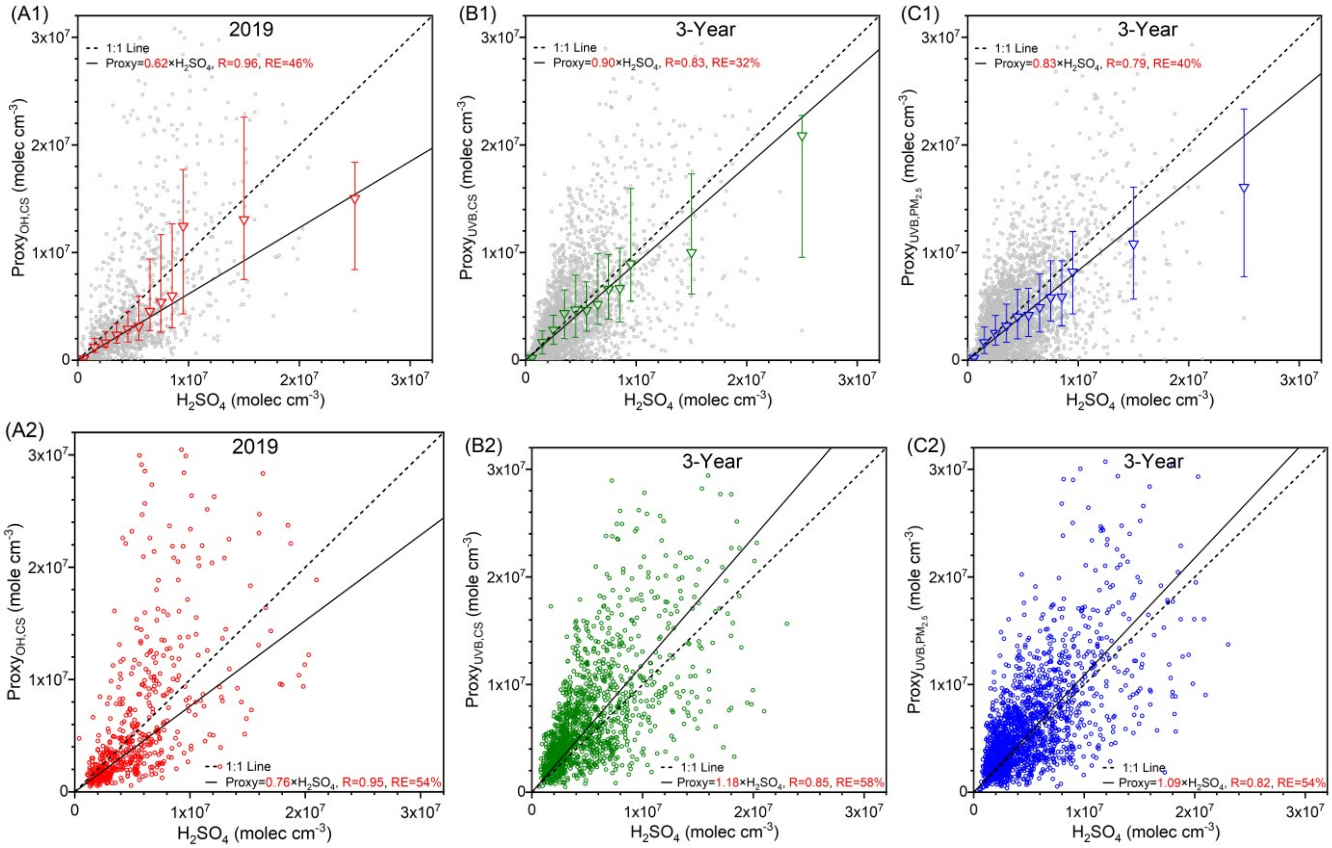

Figure S11. Sulfuric acid concentrations estimated by proxies vs. measured concentration during daytime (10:00-14:00) for (A1) and (A2) Proxy$_{OH,CS}$ in 2019, (B1) and (B2) Proxy$_{UVB,CS}$ in 3 years, and (C1) and (C2) Proxy$_{UVB,PM_{2.5}}$ in 3 years. The black dashed lines are 1:1 lines, and the black lines are the distance weighted least square fits between proxy and measured sulfuric acid. Corresponding functions of the fits, correlation coefficients (R) and relative errors (RE) are shown in the legend. For the first row, datasets include all daytime data. The triangle marker represents the binned data, where the up line, middle marker and bottom lines stand for upper quartile, median and lower quartile, respectively. For the second row, datasets only cover the optimal parameter ranges. Optimal parameter ranges for Proxy$_{OH,CS}$: 4×10^5 < [OH] < 1.2×10^7 molec cm^{-3}, 0.015 < CS < 0.07 s^{-1}, SO_2 > 0.5 ppb and RH < 60%. Optimal parameter ranges for Proxy$_{UVB,CS}$: UVB > 0.1 W m^{-2}, CS < 0.07 s^{-1}, SO_2 > 0.5 ppb and RH < 60%. Optimal parameter ranges for Proxy$_{UVB,PM_{2.5}}$: UVB > 0.1 W m^{-2}, $PM_{2.5}$ < 200 μg m^{-3}, SO_2 > 0.5 ppb and RH < 60%.

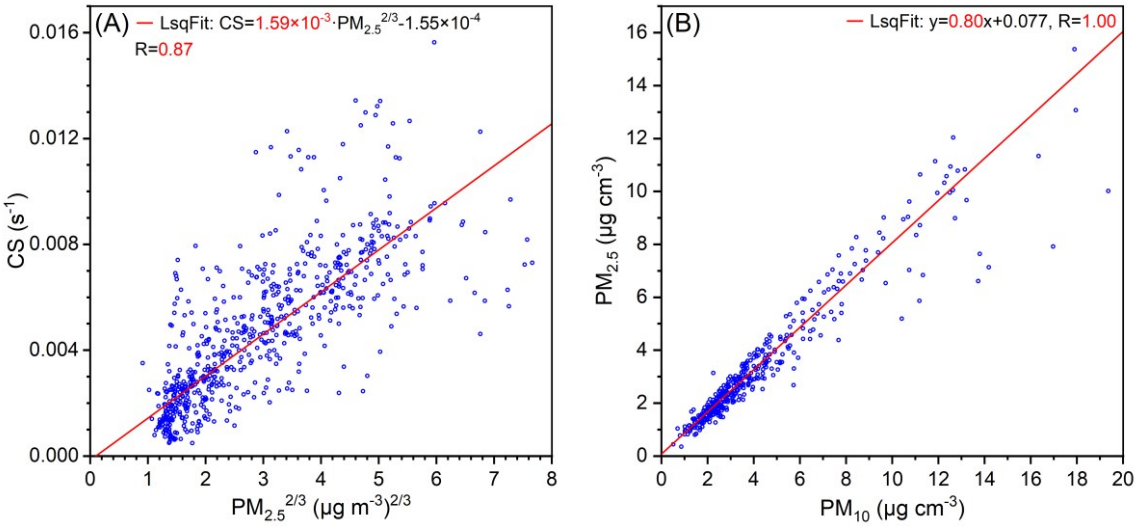

Figure S12. (A) Relationship between condensation sink (CS) and $PM_{2.5}^{2/3}$ for Hyytiälä site during daytime (10:00-14:00) from 8th March to 13th Aug. 2018. (B) Relationship between daily $PM_{2.5}$ and daily PM_{10} for Hyytiälä site from 2017 to 2019. In both two plots, the red lines are the least square fit lines between two parameters. Corresponding functions of the fits and correlation coefficients (R) are also shown in the legend.

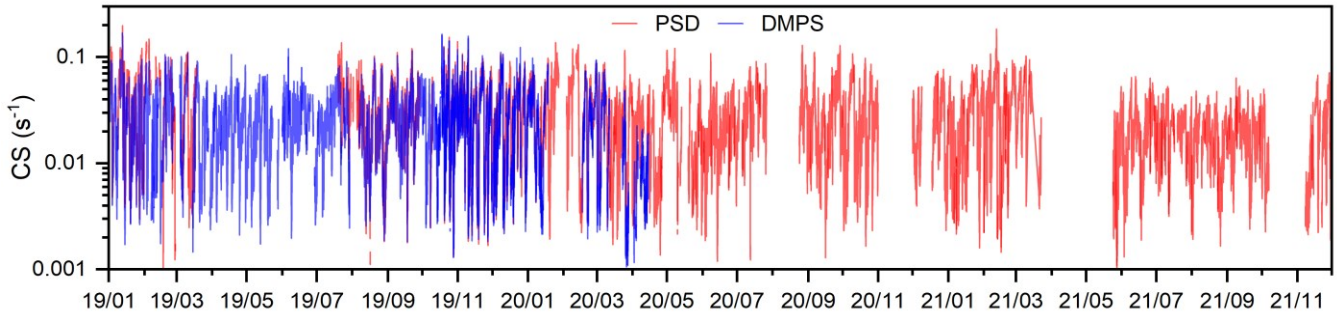

Figure S13. Three-year (from 2019 to 2021) time variations of condensation sink (CS) calculated from the particle number size distribution of PSD and DMPS. The labels on x-axes are in "year/month" format.

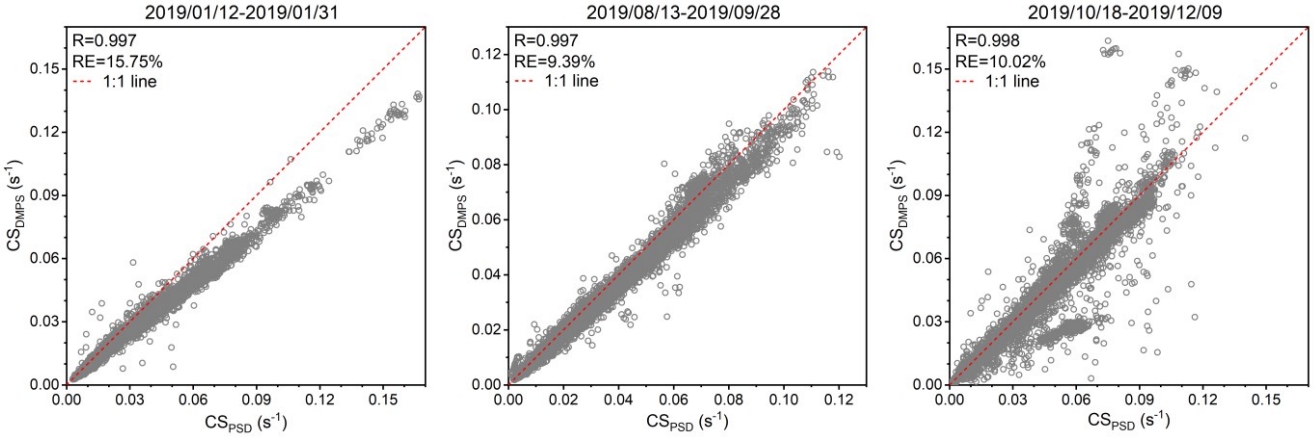

Figure S14. Correlation between condensation sinks (CS) calculated from DMPS with size ranges of 6–840 nm and PSD with size ranges of 3 nm–10 μm during three periods with continuous and stable measurement. The correlation coefficients (R) and relative errors between them are listed in the legend.

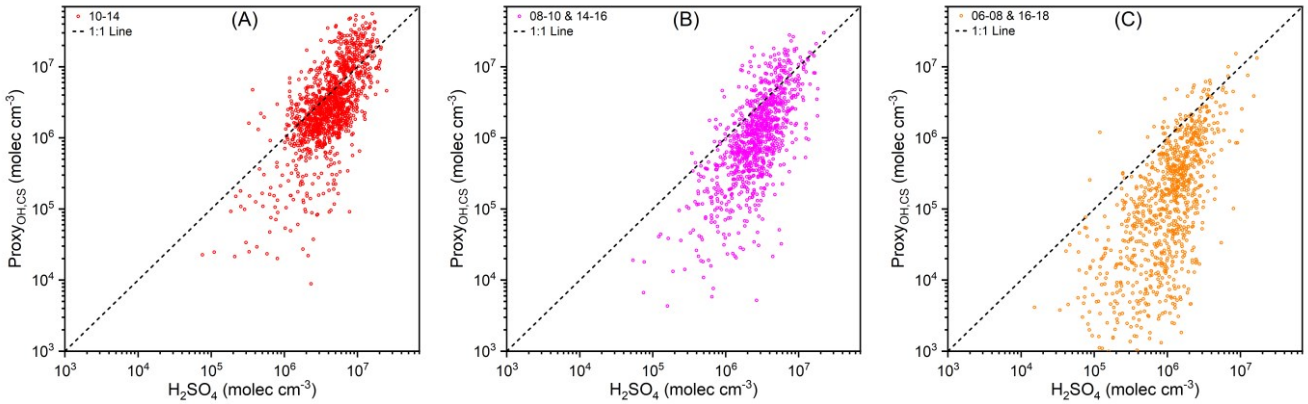

Figure S15. OH-CS based proxy vs. measured sulfuric acid during daytime in 2019 for (A) 10:00–14:00, (B) 08:00–10:00 and 14:00–16:00, as well as (C) 06:00–08:00 and 16:00–18:00. The black dashed lines are 1:1 lines.

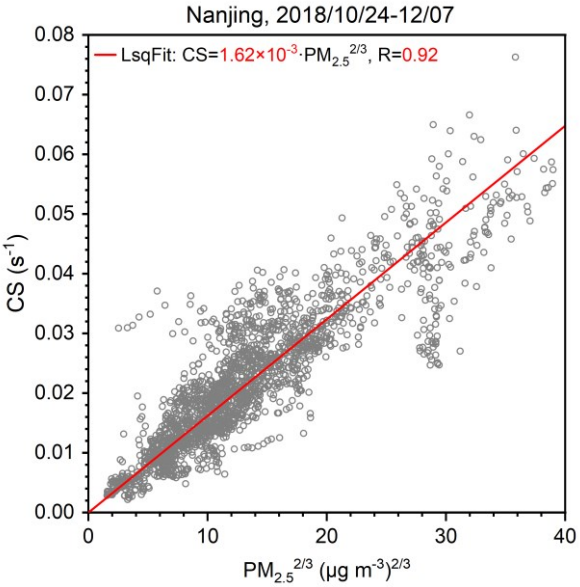

Figure S16. Relationship between condensation sink (CS) and $PM_{2.5}^{2/3}$ for Nanjing site (Nie et al., 2022) from 24th October to 7th December, 2018.

Tables

Table S1. Precipitation frequency during daytime (10:00-14:00) in May, June, July, August and September in 2019, 2020 and 2021.

Month	2019	2020	2021
May	4%	14%	8%
June	5%	15%	25%
July	**19%**	**21%**	**37%**
August	**13%**	**20%**	**26%**
September	5%	12%	24%

Table S2. Monthly concentration of H_2SO_4 (molec cm^{-3}) during nighttime (22:00-02:00 next day) from 2019 to 2021. "NaN" means there is no data available.

Month	2019			2020			2021		
	Median	25th	75th	Median	25th	75th	Median	25th	75th
January	4.7×10^5	3.2×10^5	8.3×10^5	2.8×10^5	1.8×10^5	5.4×10^5	2.6×10^5	1.7×10^5	4.8×10^5
February	4.1×10^5	2.5×10^5	6.7×10^5	2.5×10^5	1.7×10^5	4.1×10^5	3.0×10^5	2.1×10^5	4.4×10^5
March	4.0×10^5	3.2×10^5	5.2×10^5	NaN	NaN	NaN	2.3×10^5	1.6×10^5	3.8×10^5
April	2.8×10^5	1.6×10^5	4.0×10^5	2.7×10^5	1.4×10^5	4.3×10^5	2.9×10^5	2.0×10^5	4.1×10^5
May	5.0×10^5	3.3×10^5	6.4×10^5	5.1×10^5	3.8×10^5	7.6×10^5	4.5×10^5	2.9×10^5	7.0×10^5
June	3.9×10^5	2.6×10^5	5.6×10^5	5.5×10^5	3.3×10^5	7.8×10^5	4.5×10^5	2.4×10^5	5.7×10^5
July	3.4×10^5	2.4×10^5	5.0×10^5	3.3×10^5	1.7×10^5	5.2×10^5	2.9×10^5	1.7×10^5	3.9×10^5
August	3.6×10^5	2.4×10^5	6.1×10^5	4.0×10^5	3.1×10^5	5.2×10^5	3.8×10^5	2.6×10^5	5.3×10^5
September	$\mathbf{6.3\times10^5}$	4.2×10^5	8.8×10^5	4.4×10^5	2.9×10^5	6.7×10^5	NaN	NaN	NaN
October	3.5×10^5	1.8×10^5	5.6×10^5	2.9×10^5	2.1×10^5	4.1×10^5	2.5×10^5	1.4×10^5	5.3×10^5
November	2.8×10^5	1.5×10^5	5.6×10^5	2.9×10^5	1.7×10^5	4.2×10^5	2.4×10^5	1.1×10^5	5.5×10^5
December	$\mathbf{1.6\times10^5}$	9.8×10^4	7.1×10^5	2.8×10^5	1.7×10^5	4.9×10^5	NaN	NaN	NaN

Table S3. Mean, standard deviation (Std), median, lower quartile (25th) and upper quartile (75th) of sulfuric acid concentrations from measurement and estimated by proxies from literatures during the time window of 10:00-14:00 in 2019 (1st January to 31st December). The unit of concentration is molec cm^{-3}.

Parameters		Mean	Std	Median	25th	75th
Measured H_2SO_4		4.9×10^6	3.5×10^6	3.9×10^6	2.5×10^6	6.3×10^6
H_2SO_4 Proxy	Proxy $_{\text{Petäjä OH-C}}$	1.0×10^7	1.4×10^7	4.7×10^6	2.5×10^6	1.1×10^7
	Proxy $_{\text{Petäjä OH-F}}$	2.8×10^6	2.6×10^6	2.1×10^6	1.2×10^6	3.5×10^6
	Proxy $_{\text{Petäjä UVB-C}}$	7.7×10^5	8.0×10^5	5.5×10^5	2.7×10^5	1.0×10^6
	Proxy $_{\text{Petäjä UVB-F}}$	1.9×10^5	1.5×10^5	1.6×10^5	7.2×10^4	2.7×10^5
	Proxy $_{\text{Petäjä Glob-C}}$	2.1×10^6	1.8×10^6	1.7×10^6	7.4×10^5	3.0×10^6
	Proxy $_{\text{Petäjä Glob-F}}$	1.1×10^6	9.0×10^5	9.0×10^5	3.9×10^5	1.6×10^6
	Proxy $_{\text{Mikkonen et al.}}$	3.9×10^7	2.6×10^7	3.4×10^7	1.9×10^7	5.2×10^7
	Proxy $_{\text{Lu et al.}}$	8.3×10^6	3.7×10^6	7.8×10^6	5.6×10^6	1.0×10^7
	Proxy $_{\text{Dada et al.}}$	1.1×10^7	5.8×10^6	9.7×10^6	6.0×10^6	1.4×10^7

Table S4. Mean, standard deviation (Std), median, lower quartile (25th) and upper quartile (75th) of sulfuric acid concentrations from measurement and estimated by proxies in this study during daytime (10:00-14:00). The concentrations in 2019, 2020, 2021 and 3 years are summarized respectively. The unit of concentration is molec cm^{-3}.

Year	Parameters	Mean	Std	Median	25th	75th
2019	$[H_2SO_4]_{2019}$	4.9×10^6	3.5×10^6	3.9×10^6	2.5×10^6	6.3×10^6
	$Proxy_{OH,CS}$	6.0×10^6	8.2×10^6	2.8×10^6	1.5×10^6	6.3×10^6
3-Year	$[H_2SO_4]_{3\text{-}Year}$	4.4×10^6	3.3×10^6	3.5×10^6	2.1×10^6	5.8×10^6
	$Proxy_{UVB,CS}$	5.1×10^6	5.5×10^6	3.6×10^6	1.5×10^6	6.9×10^6
	$Proxy_{UVB,PM_{2.5}}$	4.5×10^6	4.7×10^6	3.2×10^6	1.3×10^6	6.1×10^6

Table S5. Performance statistics for the comparison between simulated (SIM) and observed (OBS) concentrations of NO_2, SO_2, O_3, and $PM_{2.5}$ at BUCT site during the study period (2019.1.1 – 2020.3.15).

Variables	NO_2 (ppb)	SO_2 (ppb)	$PM_{2.5}$ (μg/m^3)	O_3 (ppb)
Mean OBS	19.5	1.6	27.7	45.2
Mean SIM	17.6	1.9	28.6	40.5
Normalized Mean Bias	-10%	33%	3%	-11%
Normalized Mean Error	63%	88%	66%	57%

Table S6. Performance statistics for the comparison between simulated (SIM) and observed (OBS) concentrations of NO_2, SO_2, O_3, and $PM_{2.5}$ at national monitoring sites in China in 2019.

Variables	NO_2 (ppb)	SO_2 (ppb)	$PM_{2.5}$ (μg/m^3)	O_3 (ppb)
Mean OBS (μg/m^3)	29.3	11.3	39.2	93.3
Mean SIM (μg/m^3)	26.2	8.5	34.3	92.9
Normalized Mean Bias	-11%	-25%	-12%	0%
Normalized Mean Error	20%	27%	20%	16%

Table S7. Performance statistics for the comparison between simulated (SIM) and observed (OBS) concentrations of NO_2, SO_2, O_3, and $PM_{2.5}$ at national monitoring sites in China in 2020.

Variables	NO_2 (ppb)	SO_2 (ppb)	$PM_{2.5}$ (μg/m^3)	O_3 (ppb)
Mean OBS (μg/m^3)	26.0	10.0	34.5	91.6
Mean SIM (μg/m^3)	21.7	6.9	31.0	83.9
Normalized Mean Bias	-17%	-31%	-10%	-8%
Normalized Mean Error	28%	38%	22%	19%

Table S8. Monthly concentration of SO_2 (ppb) during daytime (10:00-14:00) from 2019 to 2021. "NaN" means there is no data available.

Month	2019			2020			2021			Annual decline using median value / %
	Median	25th	75th	Median	25th	75th	Median	25th	75th	
January	3.00	1.51	5.71	3.63	1.94	5.15	1.50	0.94	2.66	-24.9
February	2.07	0.95	4.41	1.75	0.51	3.20	2.03	1.17	3.00	-1.0
March	3.61	0.78	5.40	1.21	0.45	2.67	1.07	0.63	1.90	-35.2
April	2.08	0.79	3.54	1.88	0.47	3.94	1.02	0.36	2.08	-25.4
May	2.18	0.55	3.22	2.36	0.92	3.15	0.51	0.24	1.07	-38.3
June	1.88	0.70	3.10	0.58	0.29	1.91	0.30	0.16	0.60	-41.9
July	0.25	0.16	0.79	0.22	0.07	0.48	0.08	0.06	0.10	-34.7
August	0.36	0.28	0.87	NaN	NaN	NaN	0.23	0.18	0.32	-18.9
September	1.05	0.79	1.33	0.40	0.22	0.73	0.27	0.11	0.40	-37.0
October	0.77	0.31	1.70	0.68	0.46	1.49	0.35	0.25	0.59	-27.2
November	1.43	0.55	2.43	1.46	0.45	2.85	0.32	0.26	0.58	-39.0
December	1.46	0.75	2.30	1.75	0.98	2.66	NaN	NaN	NaN	19.3
Average										-25.4

References

Aalto, P., Hämeri, K., Becker, E., Weber, R., Salm, J., Mäkelä, J. M., Hoell, C., O'dowd, C. D., Hansson, H.-C., Väkevä, M., Koponen, I. K., Buzorius, G., and Kulmala, M.: Physical characterization of aerosol particles during nucleation events, Tellus B: Chemical and Physical Meteorology, 53, 344-358, 10.3402/tellusb.v53i4.17127, 2001.

Guo, Y., Yan, C., Li, C., Ma, W., Feng, Z., Zhou, Y., Lin, Z., Dada, L., Stolzenburg, D., Yin, R., Kontkanen, J., Daellenbach, K. R., Kangasluoma, J., Yao, L., Chu, B., Wang, Y., Cai, R., Bianchi, F., Liu, Y., and Kulmala, M.: Formation of nighttime sulfuric acid from the ozonolysis of alkenes in Beijing, Atmospheric Chemistry and Physics, 21, 5499-5511, 10.5194/acp-21-5499-2021, 2021.

Hari, P., and Kulmala, M.: Station for Measuring Ecosystem-Atmosphere Relations (SMEAR II), Boreal Environment Research, 10, 315-322, 2005.

Hari, P., Nikinmaa, E., Pohja, T., Siivola, E., Bäck, J., Vesala, T., and Kulmala, M.: Station for Measuring Ecosystem-Atmosphere Relations: SMEAR, in: Physical and Physiological Forest Ecology, edited by: Hari, P., Heliövaara, K., and Kulmala, L., Springer Netherlands, Dordrecht, 471-487, 2013.

Huang, X., Ding, A., Gao, J., Zheng, B., Zhou, D., Qi, X., Tang, R., Wang, J., Ren, C., Nie, W., Chi, X., Xu, Z., Chen, L., Li, Y., Che, F., Pang, N., Wang, H., Tong, D., Qin, W., Cheng, W., Liu, W., Fu, Q., Liu, B., Chai, F., Davis, S. J., Zhang, Q., and He, K.: Enhanced secondary pollution offset reduction of primary emissions during COVID-19 lockdown in China, Natl Sci Rev, 8, nwaa137, 10.1093/nsr/nwaa137, 2021.

Kerminen, V.-M., Pirjola, L., and Kulmala, M.: How significantly does coagulational scavenging limit atmospheric particle production?, Journal of Geophysical Research: Atmospheres, 106, 24119-24125, https://doi.org/10.1029/2001JD000322, 2001.

CUV5 and SUV Series Ultraviolet Radiometers: https://www.kippzonen.com/Product/363/SUV5-Total-UV-Radiometer.

Kulmala, M., Maso, M. D., Mäkelä, J. M., Pirjola, L., Väkevä, M., Aalto, P., Miikkulainen, P., Hämeri, K., and O'dowd, C. D.: On the formation, growth and composition of nucleation mode particles, Tellus B: Chemical and Physical Meteorology, 53, 479-490, 10.3402/tellusb.v53i4.16622, 2001.

Kulmala, M., Petäjä, T., Nieminen, T., Sipilä, M., Manninen, H. E., Lehtipalo, K., Dal Maso, M., Aalto, P. P., Junninen, H., Paasonen, P., Riipinen, I., Lehtinen, K. E. J., Laaksonen, A., and Kerminen, V.-M.: Measurement of the nucleation of atmospheric aerosol particles, Nature Protocols, 7, 1651-1667, 10.1038/nprot.2012.091, 2012.

Ma, X., Tan, Z., Lu, K., Yang, X., Liu, Y., Li, S., Li, X., Chen, S., Novelli, A., Cho, C., Zeng, L., Wahner, A., and Zhang, Y.: Winter photochemistry in Beijing: Observation and model simulation of OH and HO_2 radicals at an urban site, Science of The Total Environment, 685, 85-95, https://doi.org/10.1016/j.scitotenv.2019.05.329, 2019.

Ma, X., Tan, Z., Lu, K., Yang, X., Chen, X., Wang, H., Chen, S., Fang, X., Li, S., Li, X., Liu, J., Liu, Y., Lou, S., Qiu, W., Wang, H., Zeng, L., and Zhang, Y.: OH and HO_2 radical chemistry at a suburban site during the EXPLORE-YRD campaign in 2018, Atmospheric Chemistry and Physics, 22, 7005-7028, 10.5194/acp-22-7005-2022, 2022.

Nie, W., Yan, C., Huang, D. D., Wang, Z., Liu, Y., Qiao, X., Guo, Y., Tian, L., Zheng, P., Xu, Z., Li, Y., Xu, Z., Qi, X., Sun, P., Wang, J., Zheng, F., Li, X., Yin, R., Dallenbach, K. R., Bianchi, F., Petäjä, T., Zhang, Y., Wang, M., Schervish, M., Wang, S., Qiao, L., Wang, Q., Zhou, M., Wang, H., Yu, C., Yao, D., Guo, H., Ye, P., Lee, S., Li, Y. J., Liu, Y., Chi, X., Kerminen, V.-M., Ehn, M., Donahue, N. M., Wang, T., Huang, C., Kulmala, M., Worsnop, D., Jiang, J., and Ding, A.: Secondary organic aerosol formed by condensing anthropogenic vapours over China's megacities, Nature Geoscience, 15, 255-261, 10.1038/s41561-022-00922-5, 2022.

Tan, Z., Fuchs, H., Lu, K., Hofzumahaus, A., Bohn, B., Broch, S., Dong, H., Gomm, S., Häseler, R., He, L., Holland, F., Li, X., Liu, Y., Lu, S., Rohrer, F., Shao, M., Wang, B., Wang, M., Wu, Y., Zeng, L., Zhang, Y., Wahner, A., and Zhang, Y.: Radical chemistry at a rural site (Wangdu) in the North China Plain: Observation and model calculations of OH, HO_2 and RO_2 radicals, Atmospheric Chemistry and Physics, 17, 663-690, 10.5194/acp-17-663-2017, 2017.

TEOM 1405-D Ambient Particulate Monitor: https://www.thermofisher.cn/order/catalog/product/TEOM1405DF?SID=srch-srp-TEOM1405DF.

Thermo Scientific Model 43i-TLE: https://www.thermofisher.cn/order/catalog/product/43ITLE?SID=srch-hj-43i-TLE.

Relative Humidity and Temperature Probe HMP4: https://www.vaisala.com/en/products/instruments-sensors-and-other-measurement-devices/instruments-industrial-measurements/hmp4.

Yan, C., Shen, Y., Stolzenburg, D., Dada, L., Qi, X., Hakala, S., Sundström, A. M., Guo, Y., Lipponen, A., Kokkonen, T., Kontkanen, J., Cai, R., Cai, J., Chan, T., Chen, L., Chu, B., Deng, C., Du, W., Fan, X., He, X. C., Kangasluoma, J., Kujansuu, J., Kurppa, M., Li, C., Li, Y., Lin, Z., Liu, Y., Liu, Y., Lu, Y., Nie, W., Pulliainen, J., Qiao, X., Wang, Y., Wen, Y., Wu, Y., Yang, G., Yao, L., Yin, R., Zhang, G., Zhang, S., Zheng, F., Zhou, Y., Arola, A., Tamminen, J., Paasonen, P., Sun, Y., Wang, L., Donahue, N. M., Liu, Y., Bianchi, F., Daellenbach, K. R., Worsnop, D. R., Kerminen, V. M., Petäjä, T., Ding, A., Jiang, J., and Kulmala, M.: The effect of COVID-19 restrictions on atmospheric new particle formation in Beijing, Atmos. Chem. Phys. Discuss., 2022, 1-24, 10.5194/acp-2021-1079, 2022.

Yang, L., Nie, W., Liu, Y., Xu, Z., Xiao, M., Qi, X., Li, Y., Wang, R., Zou, J., Paasonen, P., Yan, C., Xu, Z., Wang, J., Zhou, C., Yuan, J., Sun, J., Chi, X., Kerminen, V.-M., Kulmala, M., and Ding, A.: Toward building a physical proxy for gas-phase sulfuric acid concentration based on its budget analysis in polluted Yangtze River Delta, East China, Environmental Science & Technology, 55, 6665-6676, 10.1021/acs.est.1c00738, 2021.

Zhang, R., Zhang, Y., Lin, H., Feng, X., Fu, T.-M., and Wang, Y.: NOx Emission Reduction and Recovery during COVID-19 in East China, Atmosphere, 11, 10.3390/atmos11040433, 2020.